

AMERICAN SOCIETY FOR COMPOSITES 2020 THIRTY-FIFTH TECHNICAL CONFERENCE

EDITED BY KISHORE POCHIRAJU NIKHIL GUPTA

SEPTEMBER 14–17, 2020 VIRTUAL CONFERENCE ISBN: 978-1-60595-665-7

Table of Contents

Citation

Search

Errata

MODEL-BASED DESIGN FOR MANUFACTURING

Thermo-Mechanical Characterization of a Hybrid Reinforced Photopolymer Composite via DLP 3D Printing EKUASE OKUNZUWA AUSTINE, FAREED DAWAN, PATRICK MENSAH	1056
Effect of Uniaxial Compression on the Shape Memory Behavior of Unidirectional Vitrimer Composite Embedded with Shape Memory Polymer Fibers	1071
HENRY QUANSAH AFFUL, SAMUEL IBEKWE, PATRICK MENSAH, GUOQIANG LI Evaluation of an Indirect Heating Method for Self-Healing in Shape Memory Fiber-Reinforced Polymer Composite Using High Intensity Focused Ultrasound	1086
OBINNA NWOKONKWO, GUOQIANG LI, PATRICK MENSAH, SAMUEL IBEKWE	
Sustainability of Glass Fiber Reinforced Self-healable Shape Memory Polymer Composite Laminates with Shape Memory Alloy Z-pins JOHN KONLAN, GUOQIANG LI, PATRICK MENSAH, SAMUEL IBEKWE, KAREN CROSBY	1101
Virtual Design and Demonstration of a Carbon Fiber Composite Load Floor	1122
ADAM BURLEY, GAËTAN BOIVIN, MARC-PHILIPPE TOITGANS, SELINA ZHAO, WILLIAM R. RODGERS, PRAVEEN PASUPULETI, ARNAUD DEREIMS, VENKAT AITHARAJU	
Computational Tool Development for Tailored Fiber Placement (TFP) Design Optimization	1142
DANIEL RAPKING, BERT LIU, MICHAEL BRAGINSKY, ERIC ZHOU, SCOTT HUELSKAMP, GYANESHWAR TANDON	
Artificial Neural Network Approach to Tailor Composite Materials with Nonlinear Viscoelasticity XIANBO XU, MARIAM ELGAMAL, NIKHIL GUPTA	1158
Methodology for Designing Bio-Like Structures with Diverse Geometry and Hierarchical Topologies SARAH N. HANKINS, RAY S. FERTIG, III	1171
Finite Element Analysis of 3D Woven Composites Using Consumer Graphical Processing Units BORYS DRACH	1181

Thermo-Mechanical Characterization of a Hybrid Reinforced Photopolymer Composite via DLP 3D Printing

EKUASE OKUNZUWA AUSTINE, FAREED DAWAN and PATRICK MENSAH

Abstract

The application of 3D printing in diverse industries is continuously on the increase because of its enormous benefits. However one drawback of using this techniques is the weak mechanical parts it produce. Recent studies have included carbonnanotubes (CNTs) into printed parts to improve strength using the DLP 3D techniques. Increasing the CNTs in nanocomposites decreases the mechanical properties as the CNTs absorb the UV-light irradiation meant for polymerization. This research consider basalt fillers as an alternative and CNTs/basalt hybrid reinforcement for better performance. A 5-20µm long multiwall carbon nanotube of diameter 30nm and 10µm chopped basalt fiber (BA) of diameter 10-19µm were used as the reinforcements. A commercially available Phrozen nylon-like photoresin of viscosity 7mm²/s was used as the matrix. A Phrozen Shuffle 3D printer was used to print dog-bone specimens according to tensile test standard ASTM D638 for composites. Mono-fillers composites of 0.1 wt%CNT, 0.3wt%CNT and 0.1wt%BA, 0.3wt%BA were printed. Bi-fillers composites were printed by vary the CNTs from 0.05wt% to 0.2wt% and the Basalt fiber from 0.1wt% to 0.3wt%. Fillers were mixed with the resins by ultra-sonication method. Samples were characterized by performing mechanical tests with the MTS and decomposition thermal test was performed by the TGA. The Fourier transformation infra-red spectroscopy (FTIR) was used to evaluate double bond conversion and SEM instrument was used to characterize the fractured surface of each samples. Basalt mono-filler composite had better mechanical property than CNTs mono-filler composite. Increasing the wt% of CNTs in the hybrid composite decreases the tensile strength, elastic modulus and toughness while increasing wt% of basalt filler increases these properties. Composite samples with lower wt% of fillers had higher C=C conversion as UV-light could penetrate for greater level of polymerization resulting to a stronger network. SEM image of fracture surface reveal that at lower wt% of filler, reduced pores occurs, while at high wt% of filler samples had higher pores. Composite with less wt% of filler had high initial decomposition temperature (IDT) than those with high filler wt% making them more thermally stable. Basalt composite had high initial decomposition temperature (IDT) than those of CNTs.

1. INTRODUCTION

Additive manufacturing (AM) also known as 3D printing is a manufacturing technique that produces 3D objects[1]. AM offers an efficient way of fabricating parts as it reduces material wastage and increases market responsiveness[2]. The digital light processing (DLP) 3D printing techniques, a type of vat photo polymerization (VP) AM, operates based on the curing of a photosensitive resin by exposing it to a UV-light source[3]. The resin, which is placed in a vat, is made up of acrylic monomers and photo initiator such that when expose to UV-light they begin to bond to each other to form a solid polymer through the photo polymerization process. This polymerization process occurs in three stages namely, initiation, propagation and termination [4]. Decker [5] reported that the photo initiator concentration influences the cure depth, polymerization rate and the final degree of polymerization depending on the structure and functionality of the UVcured polymer. Kim and Seo [6], studied the effect of different types and concentration of photo initiator on the mechanical properties of polyester acrylate resin. Post-curing treatment is generally recommended for parts fabricated by the VP method to improve mechanical properties[7]. Salmoria et al [8] studied the mechanical and thermal behavior as well as fractography of SLA Somos 7110 resin part post treated by different curing methods. Samples were cured at 125°C for 30mins for conventional heating and UV chamber and microwave oven for 60 and 4 mins respectively. Samples post-cured with conventional heating demonstrated improved mechanical properties than the ultraviolet and microwave post-cured. Also, in recent studies, to further improve on the mechanical and thermal properties of the DLP part, nano-fillers such as carbon nanotube have being to reinforce photopolymer to fabricate composite [9]. Sandoval et al[10] studied the interfacial bonding between the filler (MWCNT) and matrix of an epoxy-based stereolithography resin 3D printed nanocomposites. MWCNT as low as 0.05% (w/v) increase the tensile and fracture stress of the nanocomposite to 17% and 37% respectively and a further increase of the MWCNT content to 0.5% (w/v) increases the elastic modulus at temperature of about 200°C. However studies have reveal that CNTs absorb the UV-light that is meant to polymerize the resin into a stronger polymer network, hence a weak reinforced composite is formed[11].

Basalt fibers are high-performance fibers with excellent mechanical and thermal properties and are attractive replacement for glass and carbon fibers[12]. In recent literature, basalt fiber reinforced composite has being studied to prove basalt fiber has an excellent reinforced fillers [13]. Zhang et al[14] investigated the effect of continuous basalt fiber volume fraction on the mechanical and thermal properties of a poly(butylene succinate) (PBS) composite. They reported that the tensile, flexural and impact properties of the composite increases with increase in basalt fiber content. Also Basalt fiber has shown great performance in combined reinforcement with other fibers[15]. Sarasini et al[16]

investigated the impact behavior and residual properties of a basalt/carbon hybrid composites. Result indicate that the hybrid laminates of the intercalated configuration absorbed energy better and improved damage tolerance compared to the all-carbon laminates. Therefore this study evaluate chopped basalt fillers as an alternative reinforcement to CNTs in reinforcing photopolymer matrix. Additionally, the effect of basalt filler is determined in a hybrid basalt/MWCNTs reinforcement system in a Nylon-like nano composite printed with a DLP 3D AM technique. Samples of basalt (BA) reinforced composite and hybrid basalt/CNTs reinforced composite were printed and mechanically and thermally characterized.

2. EXPERIMENTAL

2.1 Materials

A commercially available acrylic based nylon-like photo curable resin (*Xiangshan Distributor*, *Hsinchu*, *Taiwan*) was used to print test samples. The photo resin has a 742 cPa.s viscosity, 130% elongation, Shore 68D Hardness and Break value of 19MPa, according to the manufacturer. A Phrozen shuffle 2018 3D printer (120mm x 68mm x 170mm) (*Xiangshan Distributor*, *Hsinchu*, *Taiwan*) was used to fabricate test samples. The printer prints with 31μm and 10μm resolution on the XY and Z axes, respectively, at a printing speed of 30 mm/hr. 500 mL of 99% purity isopropanol (*Sigma Aldrich*, *USA*) was used to rinse samples after printing. A 5-20μm long multiwall carbon nanotube (MWCNT) of diameter 30nm (*Nano lab, incorporated USA*.) and 10μm chopped basalt fiber (BA) of diameter 10-19μm (*Smarter Building Systems LLC, USA*) were used as the reinforcements.

2.2 Sample Preparation

Green pristine dog bone samples were printed with a layer thickness of 10µm and exposure time of 15 sec according to ASTM D638 (for plastic) as illustrated in Fig.1. Part of this green samples printed subjected to post curing conditions in a UV chamber with 600nm wavelength for 15 mins and then in a thermal oven for 3hrs at 100°C. Nano-Fillers were mixed with resins by sonicating for 2 hours with 30% of 500 watts of energy. Composite dog-bone specimens according to tensile test standard ASTM D638 (for composite illustrated in Fig.2) was printed for sample testing. Mono-fillers composites of 0.1 wt%CNT, 0.3wt%CNT and 0.1wt%BA, 0.3wt%BA were printed. Bi-fillers composites were printed by vary the CNTs from 0.05wt% to 0.2wt% and the Basalt fiber from 0.1wt% to 0.3wt%. Samples were further cured in a UV-chamber for 15 mins and then in an oven for 3 hrs.

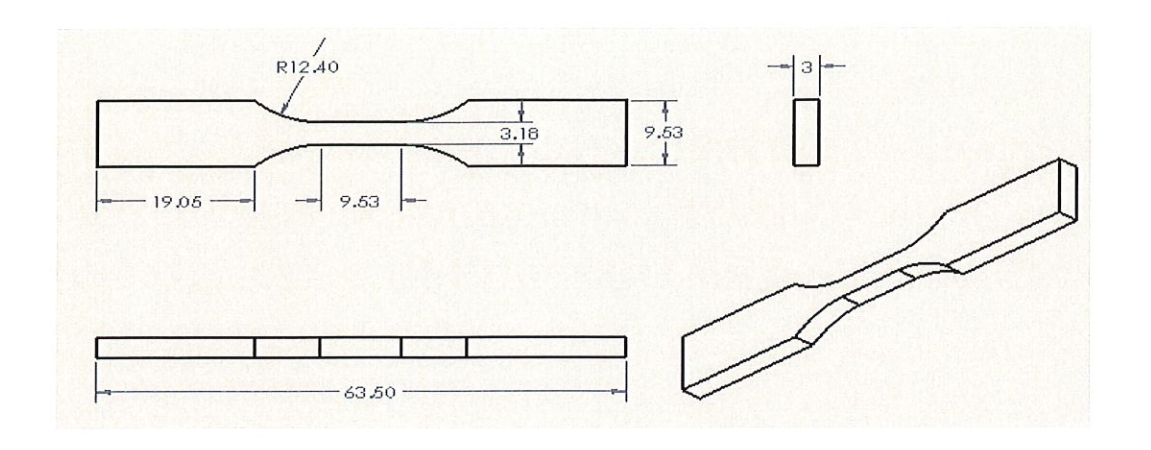


Figure 1. ASTM D638 Dog Bone Specimen Specification for Plastic (Type V).

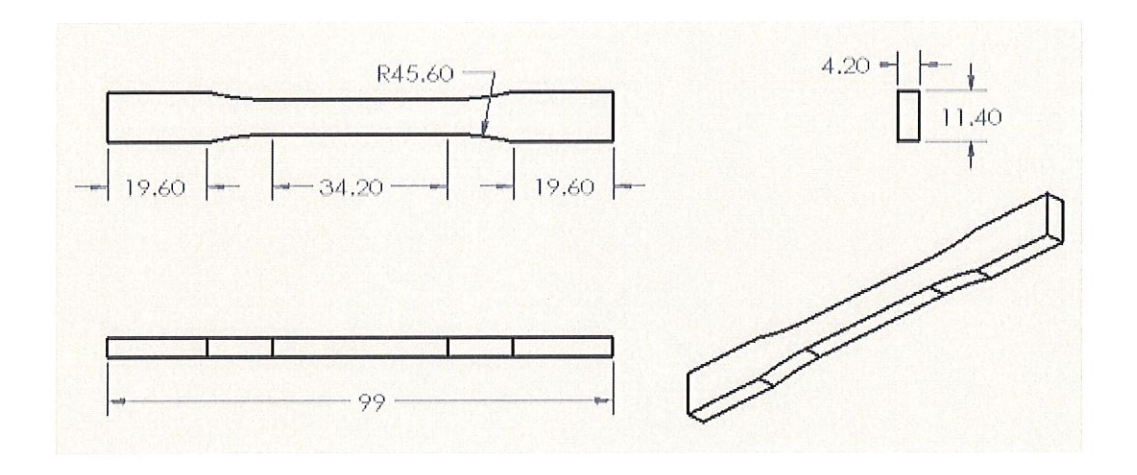


Figure 2. ASTM D638 Dog Bone Specimen Specification for Composite (Type I).

2.3 Characterization Methods

2.3.1 STRUCTURAL ANALYSIS

The FTIR spectra of the photo-resin and printed samples were determined on a Thermo Nicolet model 720X instrument (Thermo Electron Corp). The Omnic software (version 7.3) was used to record the spectra and 30 scans were conducted for each spectrum at different points of the each sample

2.3.2 TENSILE TESTING

The tensile testing was carried out in accordance with to ASTM D638 standard (both for plastic and composite) on a mechanical testing system (MTS) machine (Minnesota, USA). The strain on the cross head was set to 1mm/min and a force of 500N was applied to pull the specimen until failure occurred. An extensometer was used to measure the axial strain. The load and axial strain data were collected every 5 seconds

2.3.3 MORPHOLOGICAL CHARACTERIZATION

The fracture surface of the samples were coated with 5nm layer thickness of gold using a Desk V sputter instrument (Dentom vacuum, USA). Phenom XL scanning electron microscopy (SEM) instrument (thermo fisher scientific, USA) was used to characterized the fractured surfaces. SEM micrographs were taken at an accelerated voltage of 10kV and a magnification of 300µm.

2.3.4 THERMAL TESTING

TGA was performed using an Exstar TG/DTA7000 (Hitachi, Japan) by carrying out a decomposition reaction on 5mg of all samples in the presence of air. A constant heating rate of 10°C/min was used to ramp temperature from 30°C to 500°C and then allowed to cool to 30°C. The distribution of sample weight loss was collected by the Muse software and TGA and derivative thermogrametric analyses (DTG) was carried out with Standard software.

3. RESULTS

3.1 Mono-Filler Composite Test Result

3.1.1 FTIR TEST RESULTS

The peak absorbance of acrylate C = C stretching bond existing at 1620 cm⁻¹ to 1680cm⁻¹ wavelength was first determined for the liquid nylon resin and subsequently determined for each fabricated sample.

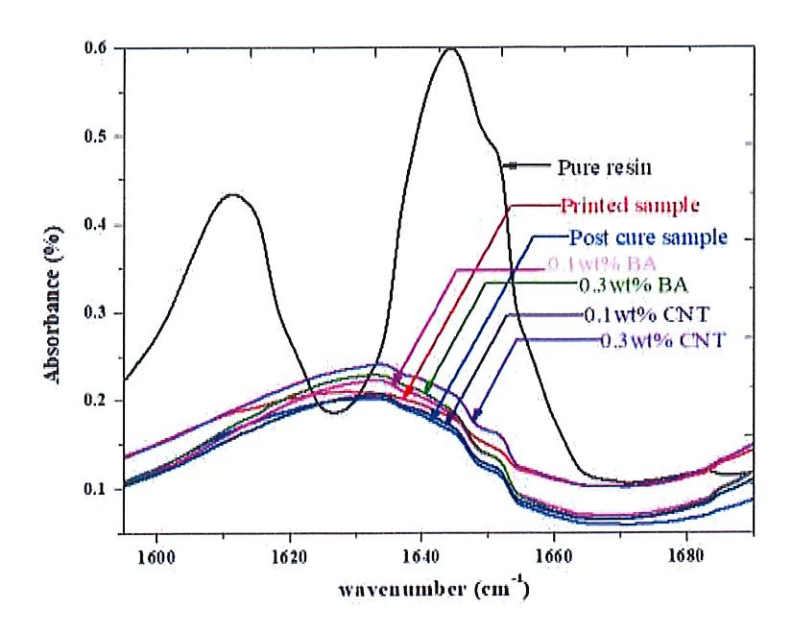


Figure 3. FTIR spectra of pure resin and various printed samples.

The green printed sample was observed to have the second lowest double bond concentration among the spectra, this is because the UV-light had un-shielded access into the resin to maximize polymerization within the allowed exposure time. On further exposure to UV-light post curing in the UV-chamber and then in the thermal oven, it was observed that the conversion of double bond continued which led to further decreased in the concentration of double bond in the post cured samples as indicated in Fig. 3. The post cured sample had the lowest double bond concentration which indicates the highest bond conversion and polymerization rate. At the same time, the spectra reveals the CNTs reinforced composites to have the highest double concentration. Also it was observed that as the wt% of CNT increases from 0.1 to 0.3, the double bond concentration in the composite increases. This can be attributed to the fact that CNTs are opaque and therefore absorbed part of the UV-light, leaving the resin matrix less UV-light for maximum polymerization. Hence there is more than usual double bond in the composite with respect to green sample. Similarly, with the basalt reinforced composite, it was observed that as the wt% of BA filler increases the double bond concentration also increases, however the bond concentration were less than that of the CNT reinforced composite. This suggest that basalt filler allows more UV-light to penetrate into the matrix resin for increase polymerization which increase the double bond conversion. This suggest that basalt fiber are translucent than their counterpart CNTs.

3.1.2 MECHANICAL TEST RESULTS

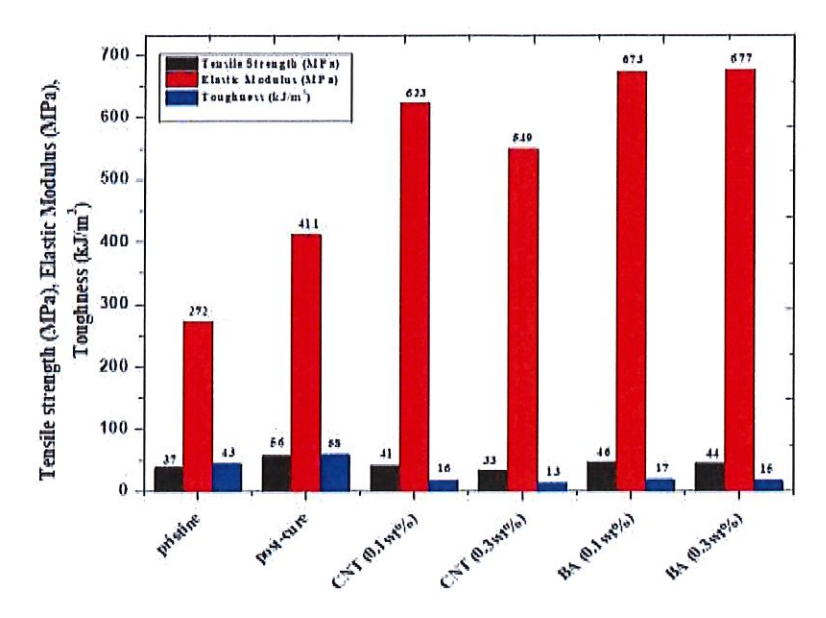


Figure 4. Mechanical test results of green and mono-filler.

Elastic Modulus

It was observed that post curing the green sample further with the post curing conditions, i.e. UV and thermal post cure, increased the elastic modulus by 50% (Fig.4). This is because post curing treatment increase the cross – linking density that exist within the polymer network. Also, incorporating filler either CNTs or BA further increased the elastic modulus by about 33% at the least performance of 0.3wt% CNT reinforced composite. This can be ascribe to the nano-fillers ability to restrict the polymer molecule from movement. It was observed that as CNTs content increases from 0.1wt% to 0.3wt%, the elastic modulus decreases from 623 MPa to 549 MPa. The significant decrease is due to the partial absorbance of the UV-light by the opaque CNTs. Conversely, increasing BA content increased the elastic modulus from 673 MPa to 677 MPa. The insignificant increase indicates the fact that although BA filler is translucent, it also prevents part of the UV-light from reaching resin matrix. Therefore, BA filler increase elastic modulus significant over CNTs as the wt% of fillers increases.

Tensile Strength

Subjecting green samples to post curing condition resulted to over 51% increase in tensile strength (Fig.4). This is because the cross-linking density network formed from the polymer chain were further locked and strengthened by post curing the samples. However incorporating nano-fillers, for example CNTs shows a significant decrease in tensile strength with at least 26% for 0.1wt% CNTs content and about 17% decrease for 0.1wt% BA content. Tensile strength for CNTs

reinforced composite decreases from 41 MPa to 33 MPa as CNT filler content increases from 0.1wt% to 0.3wt%. Similarly, the decrease of tensile strength of BA reinforced composite was seen to decline from 46 MPa to 44 MPa as BA filler wt% increases from 0.1 to 0.3. The decrease in the BA reinforced composite was insignificant compared to those of CNTs reinforced composite. It therefore means that BA filler increases the tensile strength significantly than CNT filler. This can be attributed to the high tensile strength and tensile modulus of basalt fiber as well as its translucent property.

Toughness

Post curing the pristine green samples with same condition, showed about 35% increase in the toughness of the post cured samples (Fig. 4). The increase in toughness once again shows the ability of the post curing conditions to further increase and strengthened the cross. linking network formed by the polymer chain. However comparing the percentage increase of the sample toughness to the elastic modulus and tensile strength, it was observed that the increase in toughness for post cured sample was relatively lower than the increase for elastic modulus and tensile strength. This can possibly be due to the over strengthening of the cross - link network that tend to make the samples brittle, hence toughness is compromised. For the nano-filler reinforced composite, either CNTs or BA filler, the toughness of the samples were decreased significantly with at least over 200%. This can be due to very few of the polymer chain cross—linked as the UV-light was partly shielded from maximizing polymerization within the exposure time. Also it was observed that as CNTs content increases from 0.1wt% to 0.3wt%, sample toughness decreases from 16 kJ/m³ to 13 kJ/m³ and similarly as BA content increase from 0.1wt% to 0.3wt%, toughness decreases from 17 kJ/m³ to 15 kJ/m³.

3.1.3 SEM IMAGE

The fractured surfaces of CNTs and BA reinforced composite for both 0.1wt% and 0.3wt% filler content were studied. This was done to understand the effect of each filler on the internal structure of the composite. For 0.1wt% BA content reinforcement, few pores were observed as compare to 0.3 wt% BA content (Fig.5). Meaning that as the filler particles increases in the matrix, the effect of UV-light is further reduced from completing the polymerization hence pores are formed in the sample. A similar trend was also observed in the case of CNTs reinforced composites. However the consequence of the CNTs absorbing the UV-light and preventing it from reaching the matrix was severe with the CNTs reinforcement as the nano-fillers increases with respect to BA reinforcement. For example at 0.3wt% CNTs content reinforcement, the number of pores observed did not only increased, the magnitude of the width were wider than those observed for the 0.1wt% CNTs reinforced composite as seen in Fig. 5. The formation of these pores accounts for the lack of strength in the sample material. Thus, the results from the SEM image validate the results obtained from the mechanical testing.

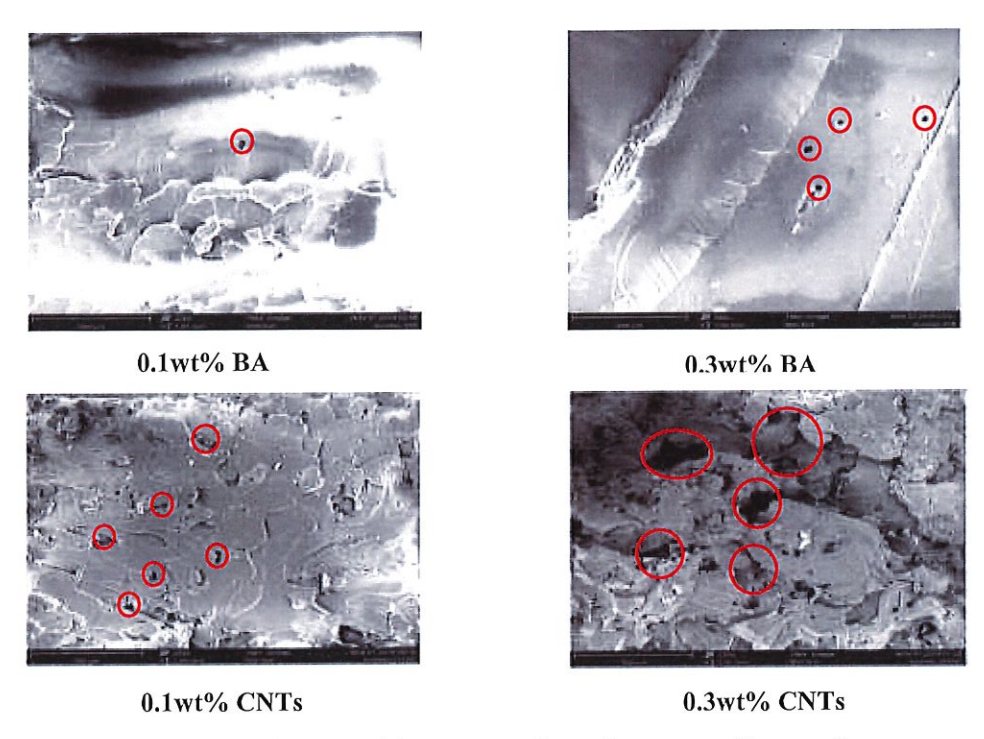


Figure 5. SEM images of fracture surfaces for composite samples.

3.1.4 THERMAL TEST RESULTS

The IDT is one of the criteria for evaluating how thermally stable a material is. It is define as the temperature at which a material first starts degrading. From Fig. 6, the green samples i.e. the pristine and post cure were observed to have the IDT of 382°C and 385°C respectively. The increase in IDT for the post cure sample over the pristine suggest that further double bond conversion, increase in cross-linking densities form by the polymer chain and strengthening of cross-linking densities occurred. However, both samples were observed to undergo two stages of weight loss from 30°C to 500°C. The first weight loss occurred between 30°C and 170°C, which may be due to lower molecular weight material[17]. While the weight loss for the second stage occurred between 310°C and 405°C which is attributed to the thermal degradation of higher cross-linking densities. The 0.1wt% BA reinforced composite was observed to have an IDT of 383°C which was closer to the value obtained for the post cure sample and greater than the pristine value. This can be attributed to the fact that basalt filler have a high thermal property and at the same translucent. Therefore the UV-light penetrates the BA filler to form and strength a higher molecular weight sample in combination with the movement restriction cause by the nano-fillers on the polymer molecules. This accounts for steady and smooth degradation observed for the BA reinforced composite (Fig.6). However as the BA filler increases to 0.3wt% this effect is reduced with the IDT reduced to 378°C. This is as a result of the attenuation of the UV-light by the presence of more BA filler in the resin matrix. As a result a reduced cross-linking densities is formed.

The CNTs reinforced composite had the lowest IDT of 376°C and 375°C for 0.1wt% and 0.3wt% CNTs respectively. Even though the CNTs are high thermal property material, they absorb the UV-light and prevent sufficient polymerization to occur to form adequate cross-linking densities among polymer chain. As a result a weak sample is formed.

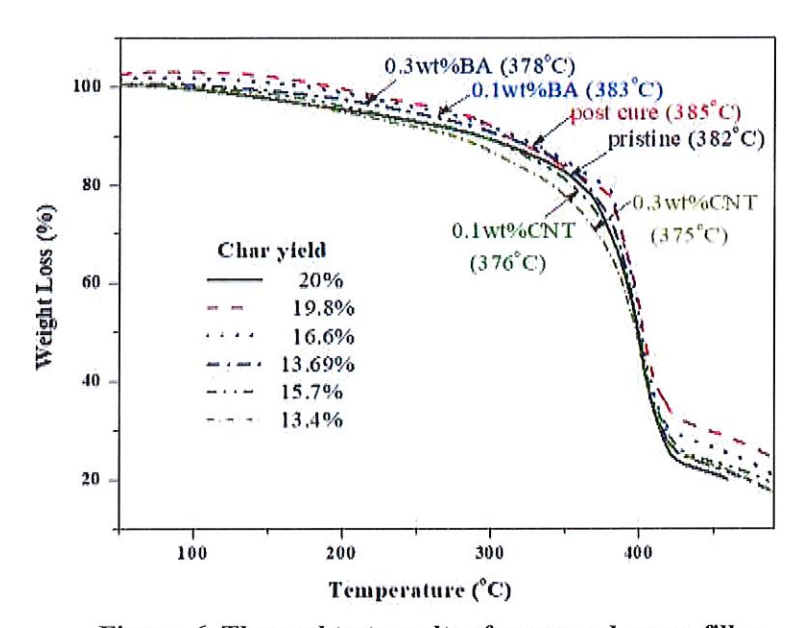


Figure. 6. Thermal test results of green and mono-filler.

The solid residue can also be refer to as the char yield. The solid residue can be used to predict the rate at which samples decomposes. The pristine and post cure samples, had the highest and about the same solid residue (20% and 19.8%), which means because of the high molecular weight formed and strengthening of the bonds, the rate at which the samples decomposes is slow. This therefore resulted in a high left over of the sample specimen. The solid residue for BA reinforced composites were less than those for the green sample and higher than those of CNTs reinforced composite for corresponding wt% filler content. This is because of the attenuated effect of UV-light from BA sample to CNTs which reduce the amount of cross-linking density formed and this reduced the molecular weight of the sample. As a result the rate at which the bonds degrades is quicker and consequently the left over solid residues is low. This correlates with the results obtain with the IDT and from the mechanical testing.

3.2 Bi-Filler Composite Test Result

3.2.1 MECHANICAL TEST RESULT

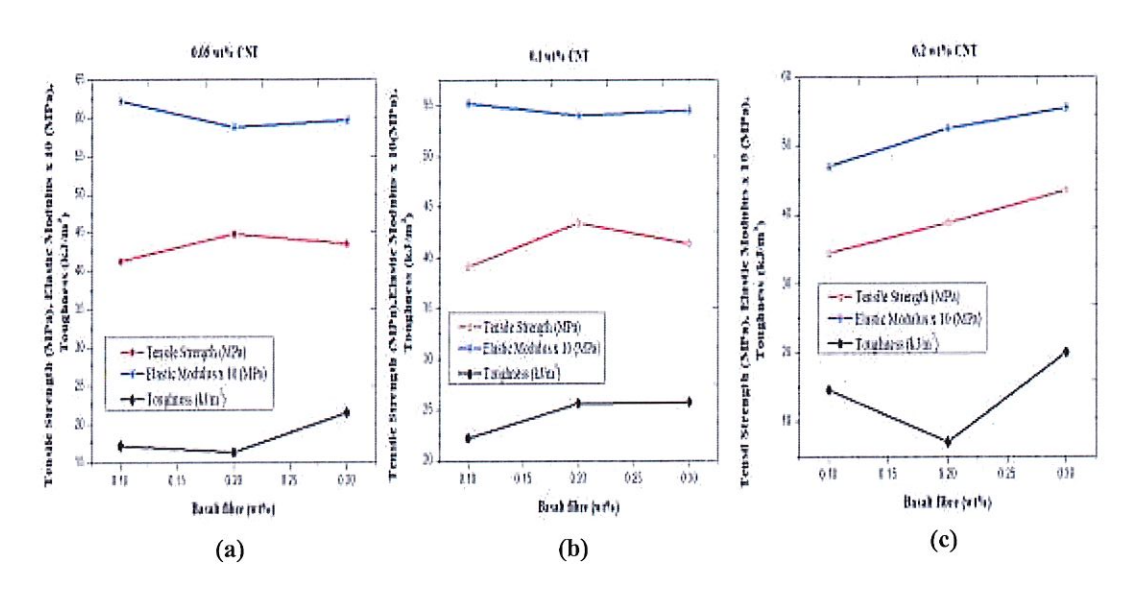


Figure 7. Mechanical properties of hybrid samples at (a) 0.05wt% CNT (b) 0.1wt% CNT (c) 0.2wt% CNT in combination with 0.1wt% - 0.3wt% BA filler.

Figure 7a, 7b & 7c present the samples characterization for 0.05wt%, 0.1wt% and 0.2wt% CNT filler as Basalt filler is increased from 0.1wt% to 0.3wt% for each wt% of CNT filler. It was observed that elastic modulus, tensile modulus and toughness decreased upon increasing the wt% of CNTs. This is most likely expected as the CNT are opaque and they absorbed the UV-light and prevent adequate curing to the polymer matrix. Hence the more they are increased in the composite the less UV-light cures the matrix. This results to less cross - linked polymer network formation in the composite that consequently brings about lack of strength. The elastic and tensile modulus shows a similar pattern for the 0.05wt% and 0.1wt% CNTs as basalt filler is increased. The elastic modulus decline and tensile strength increases as basalt filler increases. The contribution of basalt filler to the composite tensile strength can be attributed to fiber high tensile strength property. This tend to reduce the ductility of the composite which reduce the elastic property. Conversely, for the 0.2wt% CNT hybrid composite, increasing the basalt filler increased linearly both the elastic and tensile modulus. This suggests that there is a significant synergy between the CNTs and Basalt filler at higher wt% than lower wt%. This can possibly be due to the increase in the total wt% of both filler. It has being reported in literature that an increase in nano -filler wt% increase composite elastic property as a result of restriction of polymer molecule movement by nano-filler. However the optimal elastic modulus and tensile strength were observed to be 622 MPa (0.05 CNT/0.1BA) and 44.8 MPa (0.05CNT/0.2BA). These occurred with less fillers, which demonstrates that the UV and thermal post curing of the matrix to form higher cross – linked density is more significant than the effect of nano fillers in determining the mechanical strength of a photo polymerized composite. Also the optimal toughness value was observed to be 2.722 kJ/m³ (0.1CNT/0.3BA). This reflects the impact of basalt filler on the toughness in the hybrid sample as it can be observed that increasing basalt in other wt% of CNT increases the toughness of the composite

3.2.2 THERMAL TEST RESULT

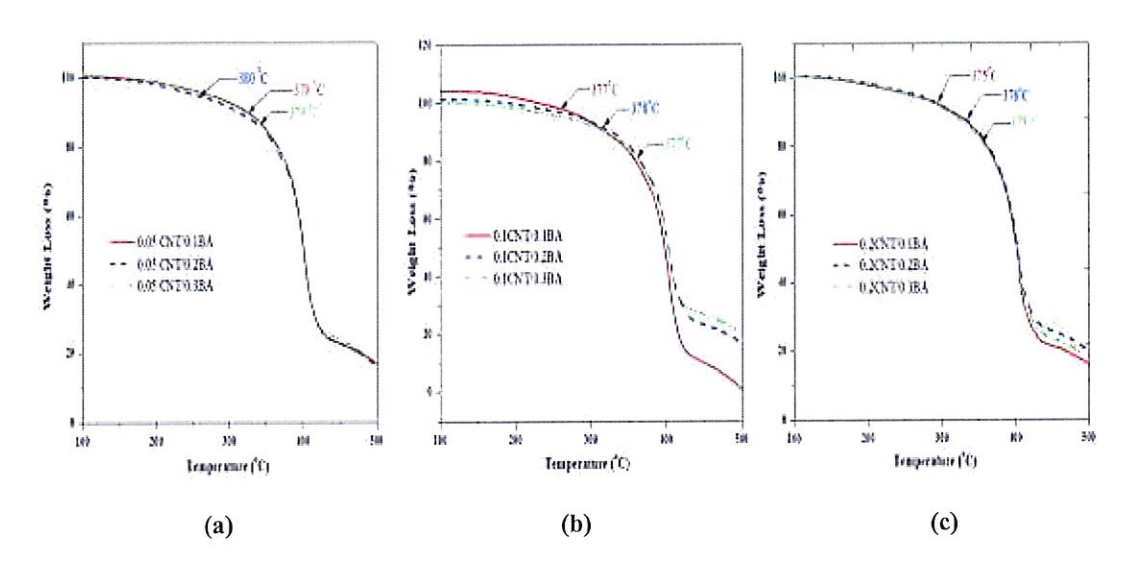


Figure 8. Thermal properties of hybrid samples at (a) 0.05wt% CNT (b) 0.1wt% CNT (c) 0.2wt% CNT in combination with 0.1wt% - 0.3wt% BA filler.

It was observed that as CNT wt% increases from 0.05wt% to 0.2wt%, the samples IDT decreases (Fig. 8a, 8b and 8c). This can be as a result of a few factors. First, as the proportion of CNTs in the hybrid composite increases, the UV-light rays is being absorbed more by the CNT rather than performing a complete polymerization on the photo matrix, hence it brings about a lower cross linking density that result to a weak sample because of incomplete polymerization. Secondly, with the increase of total fillers i.e. CNT and BA in the hybrid, the fillers shield the light from reaching the photo matrix, hence reduced cross-linking of polymer chain occurs. At the same time, as CNT wt% increases, the solid residual left after decomposition is completely increases (Table I). This suggests that the rate of decomposition of the samples decreases as CNT wt% increases. This can be attributed to CNTs as a thermally stable material which allow the conduction of heat and as a result resists the decomposition of the composite upon the application of heat. Also the increase in total fillers in the hybrid composite brings about restriction of inter-molecular movement in the polymeric matrix. This forms a bond within the material samples that slows the rate of decomposition. Therefore an increase in CNTs wt% in the hybrid composite reduces the IDT, and reduces the rate of decomposition which invariably increases the thermal stability of the composite.

Table I. Solid Residues of Hybrid composites.

Sample	Residue
0.05 CNT/0.1 BA	16.14
0.05 CNT/0.2 BA	15.60
0.05 CNT/0.3 BA	16.00
0.1 CNT/0.1 BA	0.017
0.1 CNT/0.2 BA	16.12
0.1 CNT/0.3 BA	19.45
0.2 CNT/0.1 BA	15.38
0.2 CNT/0.2 BA	19.43
0.2 CNT/0.3 BA	17.40

The effect of Basalt fillers in the hybrid composite is seen in fig. 8a, 8b, 8c with respect to thermal stability. Increasing the BA filler from 0.1wt% to 0.3wt% at different wt% of CNT shows similar pattern for the IDT and a varying pattern for the solid residue. An initial increase from 0.1wt% to 0.2wt% of BA filler resulted in an increased IDT, then a further increase of BA filler to 0.3wt% decrease the IDT. The initial rise in IDT can be attributed to the effect of increase total filler in a matrix causing restriction among the polymer chains and the thermal property of basalt filler. Also the decrease in IDT can possibly be due to the increase in total filler content shielding UV-light from forming strong bond network. The optimal basalt filler wt% for the hybrid composite with respect to the IDT was found to be 0.2wt%. On the other hand, from table 1, increasing BA filler for 0.05wt% CNT initially decreases the solid residue after decomposition and further increase results in an increase in the solid residue. This demonstrates an initial increase in decomposition rate and a later decrease as BA filler increases. Table 1 illustrate that the difference in the solid residue is not much for the samples of 0.05 wt% CNT as BA filler increases. This suggests that at lower wt% of CNT, an increase in BA fillers does not have much effect on the hybrid composite. For 0.1 wt% CNT samples, an increase in BA fillers from 0.2 wt% to 0.3wt% resulted in an increase in solid residue. Meaning there was a decrease in decomposition rate. For hybrid samples with 0.2 wt% CNT, as BA filler increase, there is an increase in solid residue i.e. decomposition rate is slowed down and with a further BA filler increase the solid residue decreases. Hence, basalt filler have much impact on the decomposition rate of the hybrid composite at higher wt% of CNT than lower wt% of CNT. This suggest a synergy effect between both fillers at higher filler wt% in the hybrid composite. The optimal hybrid sample for thermal stability was found out to have a combination of 0.1wt% CNT and 0.3wt% BA filler.

4. CONCLUSION

In this work, mono-filler reinforced composite of basalt and CNTs fillers have being printed. Also the hybrid reinforced composite of BA/CNTs with varying wt% combinations were printed. These printed composite samples were characterized by different characterization method. Base on result obtained, the following conclusion were made:

- 1. Increasing the wt% of CNT in the photo polymeric composite decreases both the mechanical and thermal properties
- 2. Basalt reinforced composite had improve mechanical and thermal properties than CNT reinforced composite
- 3. Basalt filler offers additional reinforcement to hybrid composite at an optimal 0.2 wt%
- 4. Increasing the wt% of Basalt filler increases the tensile strength and toughness of the composite at an optimal of 0.2wt%, but decreases the elastic modulus in the hybrid composite
- 5. Mono-filler reinforced photo-polymeric composite had improved elastic modulus, however hybrid composite had better tensile modulus, toughness and thermal properties.
- 6. A combination of oven and thermal cured green sample had improved mechanical and thermal properties with respect to both mono and bi-filler photo-polymeric composite with the exception of elastic modulus.

5. ACKNOWLEDGEMENT

This work was supported by the National Science Foundation through cooperative agreement OIA-154079, the Louisiana Board of Regents and NSF-CREST program award HRD 1736136.

6. REFERENCE

- [1] B. Berman, "3-D printing: The new industrial revolution," *Bus. Horiz.*, vol. 55, no. 2, pp. 155–162, 2012, doi: 10.1016/j.bushor.2011.11.003.
- [2] T. D. Ngo, A. Kashani, G. Imbalzano, K. T. Q. Nguyen, and D. Hui, "Additive manufacturing (3D printing): A review of materials, methods, applications and challenges," *Compos. Part B*, vol. 143, no. December 2017, pp. 172–196, 2018, doi: 10.1016/j.compositesb.2018.02.012.
- [3] "SLA vs. DLP: Which One Is Better? 3D Insider." https://3dinsider.com/sla-vs-dlp/(accessed Mar. 18, 2020).

- [4] B. P. Kramer and R. Jones, "Control of Free-Radical Reactivity in Photopolymerization of Acrylates," no. 4, pp. 33–41, 2012.
- [5] C. Decker and C. Decker, "Contributed papers UV-radiation curing chemistry," 2010.
- [6] D. S. Kim and W. H. Seo, "Ultraviolet-Curing Behavior and Mechanical Properties of a Polyester Acrylate Resin," no. August, 2003.
- [7] J. Binnion, "PR48 Resin."
- [8] G. V. Salmoria, C. H. Ahrens, M. Fredel, V. Soldi, and A. T. N. Pires, "Stereolithography somos 7110 resin: Mechanical behavior and fractography of parts post-cured by different methods," *Polym. Test.*, vol. 24, no. 2, pp. 157–162, 2005, doi: 10.1016/j.polymertesting.2004.09.008.
- [9] E. Fantino, A. Chiappone, F. Calignano, M. Fontana, F. Pirri, and I. Roppolo, "In situ thermal generation of silver nanoparticles in 3D printed polymeric structures," *Materials* (*Basel*)., vol. 9, no. 7, pp. 21–23, 2016, doi: 10.3390/ma9070589.
- [10] J. H. Sandoval, K. F. Soto, L. E. Murr, and R. B. Wicker, "Nanotailoring photocrosslinkable epoxy resins with multi-walled carbon nanotubes for stereolithography layered manufacturing," *J. Mater. Sci.*, vol. 42, no. 1, pp. 156–165, 2007, doi: 10.1007/s10853-006-1035-2.
- [11] J. Z. Manapat, J. D. Mangadlao, B. D. B. Tiu, G. C. Tritchler, and R. C. Advincula, "High-Strength Stereolithographic 3D Printed Nanocomposites: Graphene Oxide Metastability," ACS Appl. Mater. Interfaces, vol. 9, no. 11, pp. 10085–10093, 2017, doi: 10.1021/acsami.6b16174.
- [12] M. L. Regar and A. I. Amjad, "Bazaltna vlakna starodavna rudninska vlakna za zeleni in trajnostni razvoj," *Tekstilec*, vol. 59, no. 4, pp. 321–334, 2016, doi: 10.14502/Tekstilec2016.59.321-334.
- [13] P. I. Bashtannik, V. G. Ovcharenko, and Y. A. Boot, "Effect of combined extrusion parameters on mechanical properties of basalt fiber-reinforced plastics based on polypropylene," *Mech. Compos. Mater.*, vol. 33, no. 6, pp. 600–603, 1997, doi: 10.1007/BF02269619.
- [14] Y. Zhang *et al.*, "Mechanical and thermal properties of basalt fiber reinforced poly(butylene succinate) composites," *Mater. Chem. Phys.*, vol. 133, no. 2–3, pp. 845–849, 2012, doi: 10.1016/j.matchemphys.2012.01.105.
- [15] X. Wang, Z. Wu, G. Wu, H. Zhu, and F. Zen, "Enhancement of basalt FRP by hybridization for long-span cable-stayed bridge," *Compos. Part B Eng.*, vol. 44, no. 1, pp. 184–192, 2013, doi: 10.1016/j.compositesb.2012.06.001.
- [16] F. Sarasini *et al.*, "Drop-weight impact behaviour of woven hybrid basalt-carbon/epoxy composites," *Compos. Part B Eng.*, vol. 59, pp. 204–220, 2014, doi: 10.1016/j.compositesb.2013.12.006.
- [17] A. S. Afolabi, O. O. Sadare, and M. O. Daramola, "On the quality and performance of nanocomposite soy protein/CNTs adhesive for wood application," *Adv. Nat. Sci. Nanosci. Nanotechnol.*, vol. 7, no. 3, 2016, doi: 10.1088/2043-6262/7/3/035005.